ChemComm

COMMUNICATION

View Article Online
View Journal | View Issue

Open Access Article. Published on 28 February 2025. Downloaded on 10/19/2025 7:13:10 AM.
This article is licensed under a Creative Commons Attribution 3.0 Unported Licence.

Check for updates

Cite this: *Chem. Commun.*, 2025, **61**, 5581

Received 24th November 2024,
Accepted 24th February 2025

DOI: 10.1039/d4cc06247g

rsc.li/chemcomm

# Synthesis and characterization of triazole-functionalized mixed-valent Si(I)–Si(III) and bis(germylene) compounds†

Madhusudan K. Pandey,[a] Zohreh Hendi,[a] Xiaobai Wang,[a] Shahila Muhammed,[c] Arun Kumar,[a] Mukesh K. Singh,*[b] Regine Herbst-Irmer,[a] Dietmar Stalke,*[a] Pattiyil Parameswaran*[c] and Herbert W. Roesky*[a]

**The synthesis of mixed-valent main-group compounds is a challenging goal that has attracted significant interest recently. The reaction of 1-(2-bromophenyl)-4-phenyl-1*H*-1,2,3-triazole with $^{n}$BuLi, followed by treatment with [(PhC($^{t}$BuN)$_2$SiCl)], yielded a rare Si(I)–Si(III) compound (1), whereas treatment with [(PhC($^{t}$BuN)$_2$GeCl)] produced a bis (germylene) compound (2).**

Over the past two decades, significant advancements have been made in understanding the chemistry of heavier carbene analogues, known as tetrylenes, including silylenes and germylenes.[1] Notably, the tri-coordinated amidinato tetrylenes [PhC(N$^{t}$Bu)$_2$ECl] (E = Si[2] and Ge[3]), synthesized by Roesky and co-workers, have emerged as focal points of research. They contain divalent E(II) atoms (E = Si or Ge), with a lone pair of electrons and a vacant *p* orbital at the E(II) atoms. The past decade has seen growing interest in bi- or tridentate amidinato tetrylenes (ATs) (Fig. 1)[4] due to the excellent catalytic properties demonstrated by many transition metal complexes, especially those utilizing silylenes.[5] Amidinato tetrylenes (ATs) of types **I** and **IV**, where a donor or spacer replaces the Cl atom, are widely studied.[4] ATs of types **II** and **III**, functionalized with a donor at the N atom of the amidinate backbone, are also explored but less common.[4] In spacer-separated bis(tetrylenes) of type **IV**, two E(II) atoms are typically independent, with linkages providing sufficient space or orienting their lone pairs away from each other. Spacer-separated ATs of type **V**, with flexible spacers containing extra donor sites, can function as chelating multidentate ligands or it can bring E(II) atoms closer to show possible E···E (E = Si or Ge) interactions or E–E bond formation, are rarely investigated.[4] In this context, Driess and co-workers demonstrated that the amidinato silylene forms a hypercoordinate Si═Si dimer when the two silicon atoms are forced to come closer.[6] More recently, hetero-valent Si(IV)–Si(II) bonded silylenes have attracted significant interest due to their strong σ-donating properties, making them valuable synthons in main group and coordination chemistry.[7]

However, hetero-valent Si(I)–Si(III) bonded compounds remain scarce in the literature (Fig. 1b; **VI**). So and co-workers reported a Si(I)–Si(III) mixed-valent compound silaiminyl–silylene **VI**,[8] which Roesky and co-workers utilized recently to demonstrate interesting stimuli-induced electromerism.[9] Sen and co-workers synthesized the first amidinate-stabilized Si(II)–Si(IV) compound **VII**, featuring an unusually long

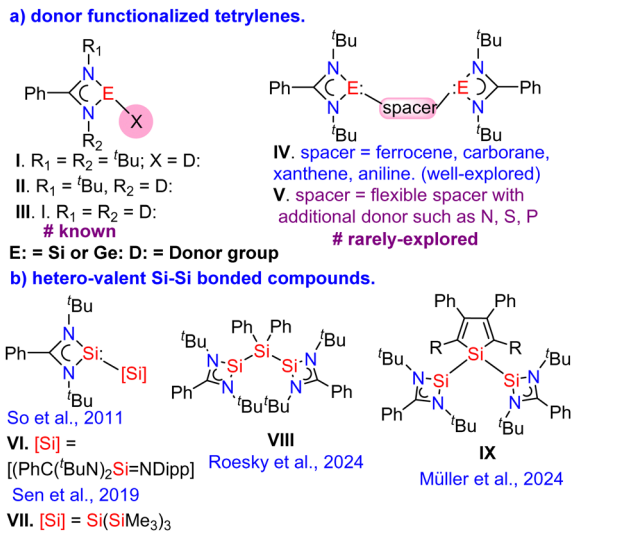


Fig. 1 (a) Selected types of known donor-functionalized tetrylenes. (b) Amidinate based hetero-valent Si–Si bonded systems. Dipp = 2, 6-diisopropylphenyl.

[a] *Institut für Anorganische Chemie, Georg-August-Universität Göttingen, Göttingen, 37077, Germany. E-mail: hroesky@gwdg.de, dstalke@chemie.uni-goettingen.de*
[b] *School of Chemistry, University of Edinburgh, Edinburgh, EH9 3FJ, UK*
[c] *National Institute of Technology Calicut, Kozhikode 673601, India. E-mail: param@nitc.ac.in*

† Electronic supplementary information (ESI) available: Experimental details and spectral data are available. CCDC 2376682 and 2376683. For ESI and crystallographic data in CIF or other electronic format see DOI: **https://doi.org/10.1039/d4cc06247g**

Open Access Article. Published on 28 February 2025. Downloaded on 10/19/2025 7:13:10 AM.
This article is licensed under a Creative Commons Attribution 3.0 Unported Licence.

Si(II)–Si(IV) bond distance of 2.4339(13) Å,[10] which afforded unsymmetrical $sp^2$–$sp^3$ disilenes upon treatment with aliphatic chlorophosphines.[11] More recently, Roesky and co-workers developed a unique bis(silylene) **VIII** with a Si(II)–Si(IV)–Si(II) bonding arrangement, exhibiting Si(II)–Si(IV) bond distances of 2.4212(8) Å and 2.4157(7) Å and explored its coordinating ability with Fe(0).[12a] Driess and co-workers employed **VIII** to activate the C≡O bonds of carbon monoxide under ambient conditions (1 atm, room temperature), leading to the formation of 1,3-disilacyclopentadiene.[12b] Müller and co-workers reported a bis(silylene)silole **IX** with Si(II)–Si(IV) bond distances of 2.4590(6) Å and 2.4635(5) Å and explored its reactivity with chalcogenide and organic azides.[13] These examples underscore the significance of hetero-valent Si–Si bonded silylenes in both main group and coordination chemistry. Despite extensive research on functionalized triazoles with P, Se donors, their functionalization with tetrylene moieties remains unexplored.[14] Incorporating heteroaryl groups with donor atoms like nitrogen, oxygen, or sulfur near tetrylene moieties can create versatile ligand systems with rich coordination chemistry, suitable for applications in homogeneous catalysis, molecular switches, logic gates, and sensors. We envisioned that the triazole functionalized E2 systems would not only provide a versatile ligand system but might also bring the E(II) atoms in close proximity to afford versatile mixed-valent E–E bonded compounds. Herein, we report the reaction of dilithiated triazole with amidinato tetrylenes [PhC(N$^t$Bu)$_2$ECl] (E = Si and Ge) resulting in the formation of a rare Si(I)–Si(III) bonded compound **1** and a bis(germylene) compound **2**, respectively.

The reaction of 1-(2-bromophenyl)-4-phenyl-1*H*-1,2,3-triazole[14b] with two equivalents of $^n$BuLi at −80 °C in diethyl ether followed by treatment with two equivalents of [(PhC($^t$BuN)$_2$SiCl)][2b] resulted in the formation of a rare mixed valent Si(I)–Si(III) compound **1** as dark yellow crystalline solid in good yield, instead of the anticipated bis(silylene) compound **1′** (Scheme 1).[14c,d] Whereas, the reaction of 1-(2-bromophenyl)-4-phenyl-1*H*-1,2,3-triazole with two equivalents of $^n$BuLi followed by treatment with two equivalents of amidinato germylene chloride [(PhC($^t$BuN)$_2$GeCl)][3] afforded triazole fused bis(germylene) compound **2** as a colorless solid in good yield (Scheme 1). Both compounds were thoroughly characterized using various spectroscopic techniques and are highly stable in both solution and solid states for months without decomposition when stored under argon. The $^{29}$Si NMR spectrum of **1** in $C_6D_6$ showed two singlet resonances at 46.52 and −94.22 ppm, corresponding to Si(I) and Si(III) atoms (see ESI,† Fig. S3). The $^{29}$Si NMR resonance for the Si(I) atom in **1** is downfield shifted compared to the same in silaiminyl–silylene **VI** ($\delta$ = 31.8 ppm for Si(I) atom)[9] and upfield shifted compared to [(PhC($^t$BuN)$_2$Si)]$_2$ ($\delta$ = 76.29 ppm).[15] This suggests that the Si(III) fragment of silaiminyl–silylene **VI** is a better donor than the triazole and amidinate stabilized Si(III) fragment in **1**, resulting in a downfield shift in the $^{29}$Si NMR spectrum of Si(I) atom in **1**. The $^1$H NMR spectrum of **1** showed three distinct singlet resonances at 0.68, 0.78 and 1.22 ppm for $^t$Bu protons with an integral ratio of 1 : 1 : 2, suggesting the formation of **1**. Further, LIFDI mass spectrometry confirmed the molecular composition, which showed [M + H]$^+$ molecular ion mass at 738.3. The $^1$H NMR spectrum of **2** suggested a bis(germylene) compound formation with two distinct singlet resonances for the $^t$Bu protons of the amidinate at 0.96 and 1.10 ppm. The aromatic protons appeared in the range of 6.99 to 8.32 ppm. Further, the high-resolution mass spectrometry showed a molecular ion peak at 828.3039 for [M + H]$^+$ ion (calcd 828.3040), and the molecular structure was established using X-ray diffraction study.[16] The molecular structures of **1** and **2** are shown in Fig. 2 and 3, and the selected bond lengths and bond angles are listed in the captions of the figure.

Compounds **1** and **2** crystallized in the monoclinic $P2_1/n$ and triclinic $P\bar{1}$ space groups, respectively. The molecular structure of **1** confirms the formation of a rare Si(I)–Si(III) bonded mixed valent compound with a Si1–Si2 bond length of 2.4458(8) Å (Fig. 2). The Si(I) atom has a distorted trigonal pyramidal geometry with an amidinate ligand occupying two sites and

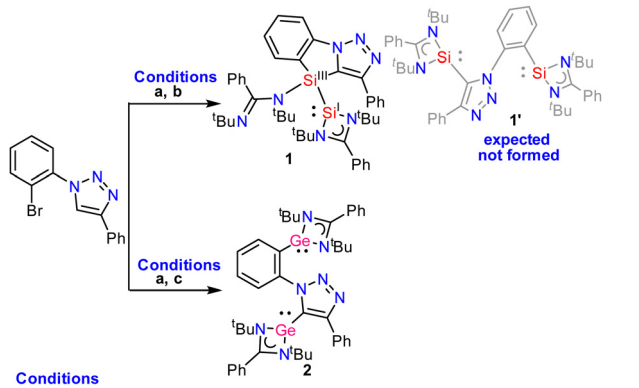


Scheme 1 Synthesis of **1** and **2**.

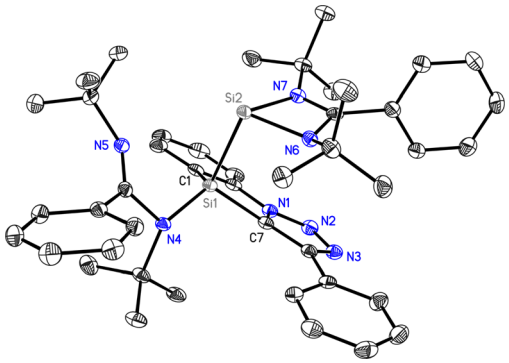


Fig. 2 Molecular structure of **1**. The anisotropic displacement parameters are drawn at 50% level. All the hydrogen atoms have been omitted for clarity. Selected bond lengths [Å] and bond angles [°]: Si1–Si2 2.4458(8), Si1–C1 1.8997(17), Si1–C7 1.9100(17), Si1–N4 1.7687(14), Si2–N6 1.8789(14), Si2–N7 1.8782(14), N4–Si1–C1 116.37(7), N4–Si1–C7 112.95(7), C1–Si1–C7 87.73(7), N4–Si1–Si2 113.62(5), C1–Si1–Si2 115.31(5), C7–Si1–Si2 107.77(5), N7–Si2–N6 69.67(6), N7–Si2–Si1 98.20(5), N6–Si2–Si1 102.51(5).

Open Access Article. Published on 28 February 2025. Downloaded on 10/19/2025 7:13:10 AM.
This article is licensed under a Creative Commons Attribution 3.0 Unported Licence.

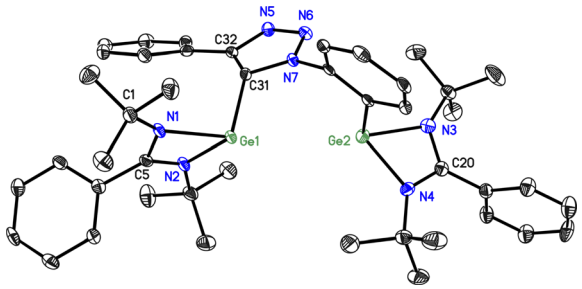


Fig. 3 Molecular structure of **2**. Anisotropic displacement parameters are drawn at 50% probability level. Selected bond lengths [Å] and bond angles [°]: Ge1–N1 2.001(2), Ge1–N2 2.009(2), Ge2–N3 2.003(2), Ge2–N4 2.014(2), Ge1–C31 2.039(3), Ge2–C44 2.026(3), N1–Ge1–N2 65.46(9), N3–Ge2–N4 65.26(9), N1–Ge1–C31 104.50(9), N2–Ge1–C31 98.67(9), N3–Ge2–C44 96.78(10), N4–Ge2–C44 96.06(10).

the lone pair of electrons residing on the apex. The Si(III) atom has a four-coordinate tetrahedral arrangement with a bis-chelate triazole core occupying two coordination sites, forming a five-membered heterocyclic ring. The N and Si atoms of amidinate and silylene occupied the other two sites of the tetrahedron. The sum of the bond angles around the Si(1) atom (270.38°) and the angle between the centroid of the $CN_2Si$ plane and the Si(I)–Si(III) bond (104.2°) suggest the stronger s-character of the lone pair at Si(1). The Si1–Si2 bond length of 2.4458(8) Å in **1** is longer than the Si–Si bond length in interconnected amidinato bis(silylene) $[PhC(N^tBu)_2Si]_2$ [2.413(2) Å], bis(silylene) **VIII** with Si(II)–Si(IV) bond distances of 2.4212(8) Å and 2.4157(7) Å and is slightly shorter in bis(silylene)silole **IX** with Si(II)–Si(IV) bond distances of 2.4590(6) and 2.4635(5) Å.[12,13,15] The molecular structure of compound **2** reveals that the Ge atoms adopt a distorted trigonal pyramidal geometry, with bond angles summing to 268.63° (Ge1) and 258.1° (Ge2). A Ge···Ge distance of 4.205 Å in **2** also rules out any significant bonding interaction, which confirms the formation of a spacer-separated bis(germylene) compound (Fig. 3). Interestingly, the distances between Ge1···Ge2 and Ge1···N6 atoms are 4.205 and 3.355 Å, suggesting the bis(germylene) compounds might serve as chelating multidentate ligands (see ESI,† Fig. S9).

We gained insight into the structural, bonding, and difference in reactivity aspects for both **1** and **2** through quantum chemical Density Functional Theory (DFT) calculations (please see ESI† for computational details). We hypothesize that the reaction of the dilithiated triazole with amidinato-silylene/germylene chlorides results in bis(silylene) (**1′**) or bis-germylene (**2**) (Fig. 4). However, we could not isolate bis(silylene) **1′** and always obtained a mixed-valent Si(I)–Si(III) bonded compound **1**. The molecular orbital analysis (Fig. 4 and Fig. S12, ESI†) indicates that the highest occupied molecular orbital (HOMO) of bis-silylene (**1′**)/bis-germylene (**2**) are lone pair orbitals on the Group-14 element connected with the phenyl ring. Since the s-character of lone pair orbital on the germanium centre in **2** is more as compared to that of the silicon centre in **1′**, the latter one is more reactive. This is corroborated by the eigenvalue of HOMO of **2** (−5.58 eV) and **1′** (−4.39 eV). On the other hand, the lowest unoccupied orbitals (LUMO) are the E–N σ* orbital in conjugation with the π-orbital

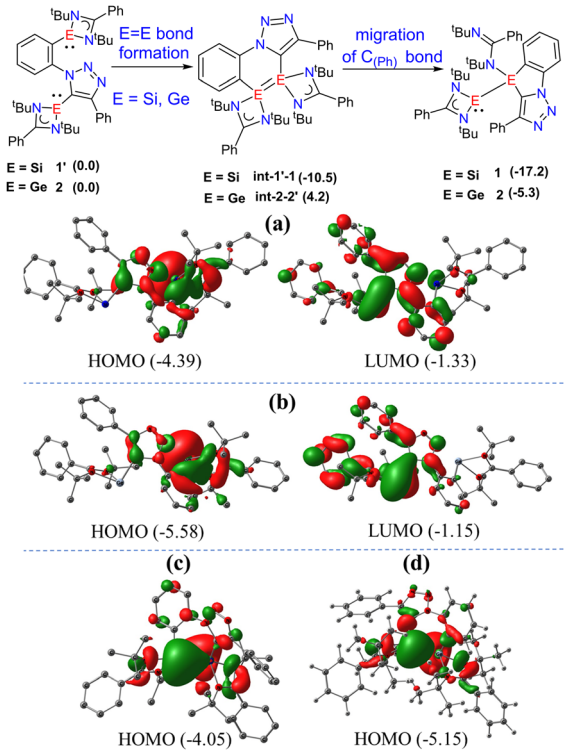


Fig. 4 Calculated reaction energetics for the formation of products from triazole as shown in Scheme 1 and the important molecular orbitals – (a) HOMO and LUMO of **1′**, (b) HOMO and LUMO of **2**, (c) HOMO of **int-1′-1**, (d) HOMO of **int-2-2′**. The calculations are carried out at M06/def2-TZVPP//BP86-D3(BJ)/def2-SVP level of theory. Surfaces are plotted at the iso-surface value of 0.03.

of the triazole ring, which is slightly more stabilized for **1′** (−1.33 eV) as compared to that of **2** (−1.15 eV). Consequently, the intramolecular rearrangement by the coordination of lone pair orbital of heavier Group-14 centre connected to the phenyl ring with the E–N σ* orbital of the other Group-14 centre connected to the triazole ring leads to disilene **int-1′-1** and digermene **int-2-2′**. Since the silicon lone pair and the Si−N σ* orbital is more reactive as compared to the germanium lone pair and the Ge–N σ* orbital, the formation of **int-1′-1** (−10.5 kcal $mol^{-1}$) is exergonic and the formation of **int-2-2′** is endergonic (4.2 kcal $mol^{-1}$). Note that Driess and coworkers isolated a similar derivative of disilene **int-1′-1**.[6] The HOMO of the disilene **int-1′-1** and the digermene **int-2-2′** are pseudo-π-MO formed by the overlap of E−N σ* orbitals of tetrylene fragments having pseudo-π-symmetry. These pseudo-π-MOs (−4.05 eV for **int-1′-1** and −5.15 eV for **int-2-2′**) lie higher in energy than the lone pair orbitals of **1′** and **2**. The phenyl carbon bonded to the heavier Group-14 centre is more electrophilic ($q$ = 0.05 $e$) than the triazole carbon ($q$ = −0.29 $e$) bonded to the other heavier Group-14 centre. Hence, the pseudo-π-MO is susceptible to donate into the Si–C σ*-orbital leading to the migration of the phenyl ring accompanied by Si–N bond cleavage. The higher stability of **1** and **2** can be attributed to the higher stability of the lone pair compared to the pseudo-π-MO.

Open Access Article. Published on 28 February 2025. Downloaded on 10/19/2025 7:13:10 AM.
This article is licensed under a Creative Commons Attribution 3.0 Unported Licence.

Using Ahlrichs–Heinzmann population analysis,[17] we found two types of Si atoms (Si(III) and Si(I)), with partial charge of 0.25 and 0.08, respectively. To better understand the Si–Si interaction in **1**, we carried out natural bonding orbitals (NBO)[18] and quantum theory of atoms in molecules (QTAIM)[19] analysis. NBO-based bonding orbital shows a strong interaction between $Si1(3s^{0.33}3p_z^{0.67})^{0.61}$ and $Si2(3s^{0.15}3p_z^{0.85})^{0.39}$, with an occupancy of 1.79 (Fig. S14c, ESI†). Further, Wiberg bond index (WBI) calculation,[20] which gives information about the bond order between two questioned atoms, suggests a bond between both Si atoms (0.83). The molecular graph plotted from DFT-QTAIM analysis displays a bond critical point (3,−1) between Si–Si with an electron density of $\rho = 0.0771e$ Bohr$^{-3}$, Laplacian of electron density ($\nabla^2\rho(r)$) $-0.1078e$ Bohr$^{-5}$ and energy density ($H(r)$) $-0.3501e$ Bohr$^{-3}$ (Fig. S14d and e, ESI†).[21] The large value of $\rho$ and negative values for both $\nabla^2\rho(r)$ and $H(r)$ suggest a strong covalent bond between Si1···Si2. Additionally, the localized orbital locator (LOL) graph (Fig. S14f, ESI†) highlights a highly localized region between both Si centres, indicating the presence of the Si–Si bond.

In conclusion, we successfully synthesized and characterized two novel compounds: a rare mixed-valent Si(I)–Si(III) compound (**1**) and a bis(germylene) compound (**2**). In compound **2**, the long interatomic distances (Ge1···Ge2 = 4.205 Å and Ge1···N6 = 3.355 Å) indicate the absence of significant Ge···Ge interaction, which maybe suggest its potential as a versatile multidentate ligand in coordination chemistry.

M. K. P.: conceptualization, data curation, formal analysis, investigation, writing – original draft, review & editing, visualization, Z. H.: data curation, formal analysis, writing – review & editing, X. W.: single-crystal measurement, S. M.: DFT calculations, writing – review & editing, A. K.: writing – review & editing, M. K. S.: NBO and QTAIM analysis, R. H.-I.: supervision, D. S.: supervision, writing – review & editing, P. P.: supervision, writing – review & editing, H. W. R.: writing – review & editing, supervision, funding acquisition.

## Data availability

The NMR, mass and DFT calculation data that support the findings of this work have been included in the ESI.† Crystallographic data for **1** and **2** has been deposited at the Cambridge Crystallographic Data Centre (CCDC) under deposition number 2376682 (**1**) and 2376683 (**2**) and can be obtained from **https://www.ccdc.cam.ac.uk/structures/**.

## Conflicts of interest

There are no conflicts to declare.

## Notes and references

1 (*a*) S. Nagendran and H. W. Roesky, *Organometallics*, 2008, **27**, 457–492; (*b*) S. S. Sen, S. Khan, P. P. Samuel and H. W. Roesky, *Chem. Sci.*, 2012, **3**, 659–682; (*c*) L. Wang, Y. Li, Z. Li and M. Kira, *Coord. Chem. Rev.*, 2022, **457**, 214413; (*d*) Y. Mizuhata, T. Sasamori and N. Tokitoh, *Chem. Rev.*, 2009, **109**, 3479–3511; (*e*) M. S. Nechaev, *Organometallics*, 2021, **40**, 3408–3423.
2 (*a*) C.-W. So, H. W. Roesky, J. Magull and R. B. Oswald, *Angew. Chem., Int. Ed.*, 2006, **45**, 3948–3950; (*b*) S. S. Sen, H. W. Roesky, D. Stern, J. Henn and D. Stalke, *J. Am. Chem. Soc.*, 2010, **132**, 1123–1126.
3 S. Nagendran, S. S. Sen, H. W. Roesky, D. Koley, H. Grubmüller, A. Pal and R. Herbst-Irmer, *Organometallics*, 2008, **27**, 5459–5463.
4 (*a*) J. A. Cabeza and P. García-Álvarez, *Chem. – Eur. J.*, 2024, **30**, e202400786; (*b*) Z. Hendi, M. K. Pandey, K. Rachuy, M. K. Singh, R. Herbst-Irmer, D. Stalke and H. W. Roesky, *Chem. – Eur. J.*, 2024, **30**, e202400389; (*c*) M. K. Pandey, Z. Hendi, X. Wang, A. Bhandari, M. K. Singh, K. Rachuy, S. Kumar Kushvaha, R. Herbst-Irmer, D. Stalke and H. W. Roesky, *Angew. Chem., Int. Ed.*, 2024, **63**, e202317416.
5 (*a*) B. Blom, M. Stoelzel and M. Driess, *Chem. – Eur. J.*, 2013, **19**, 40–62; (*b*) B. Blom, D. Gallego and M. Driess, *Inorg. Chem. Front.*, 2014, **1**, 134–148; (*c*) Z. Hendi, M. K. Pandey, S. K. Kushvaha and H. W. Roesky, *Chem. Commun.*, 2024, **60**, 9483–9512; (*d*) C. Shan, S. Yao and M. Driess, *Chem. Soc. Rev.*, 2020, **49**, 6733–6754; (*e*) M. Ghosh and S. Khan, *Dalton Trans.*, 2021, **50**, 10674–10688.
6 A. Kostenko and M. Driess, *J. Am. Chem. Soc.*, 2018, **140**, 16962–16966.
7 (*a*) A. V. Protchenko, A. D. Schwarz, M. P. Blake, C. Jones, N. Kaltsoyannis, P. Mountford and S. Aldridge, *Angew. Chem., Int. Ed.*, 2013, **52**, 568–571; (*b*) M. M. D. Roy, M. J. Ferguson, R. McDonald, Y. Zhou and E. Rivard, *Chem. Sci.*, 2019, **10**, 6476–6481; (*c*) D. Reiter, R. Holzner, A. Porzelt, P. J. Altmann, P. Frisch and S. Inoue, *J. Am. Chem. Soc.*, 2019, **141**, 13536–13546.
8 S.-H. Zhang, H.-W. Xi, K. H. Lim, Q. Meng, M.-B. Huang and C.-W. So, *Chem. – Eur. J.*, 2012, **18**, 4258–4263.
9 R. Yadav, X. Sun, R. Köppe, M. T. Gamer, F. Weigend and P. W. Roesky, *Angew. Chem., Int. Ed.*, 2022, **61**, e202211115.
10 M. K. Bisai, V. S. V. S. N. Swamy, T. Das, K. Vanka, R. G. Gonnade and S. S. Sen, *Inorg. Chem.*, 2019, **58**, 10536–10542.
11 M. K. Bisai, T. Das, K. Vanka, R. G. Gonnade and S. S. Sen, *Angew. Chem., Int. Ed.*, 2021, **60**, 20706–20710.
12 (*a*) S. K. Kushvaha, P. Kallenbach, S. M. N. V. T. Gorantla, R. Herbst-Irmer, D. Stalke and H. W. Roesky, *Chem. – Eur. J.*, 2024, **30**, e202303113; (*b*) S. Yao, M. S. Budde, X. Yang, Y. Xiong, L. Zhao and M. Driess, *Angew. Chem., Int. Ed.*, 2024, e202414696.
13 C. Liu, M. Schmidtmann and T. Müller, *Dalton Trans.*, 2024, **53**, 10446–10452.
14 (*a*) D. Mondal and M. S. Balakrishna, *Eur. J. Inorg. Chem.*, 2020, 2392–2402; (*b*) B. Choubey, L. Radhakrishna, J. T. Mague and M. S. Balakrishna, *Inorg. Chem.*, 2016, **55**, 8514–8526; (*c*) F. E. Bugden, G. J. Clarkson and M. D. Greenhalgh, *Eur. J. Org. Chem.*, 2023, e202201459; (*d*) L. Radhakrishna, M. K. Pandey and M. S. Balakrishna, *RSC Adv.*, 2018, **8**, 25704–25718.
15 S. S. Sen, A. Jana, H. W. Roesky and C. Schulzke, *Angew. Chem., Int. Ed.*, 2009, **48**, 8536–8538.
16 (*a*) Bruker AXS Inc., Madison, 2016; (*b*) L. Krause, R. Herbst-Irmer, G. M. Sheldrick and D. Stalke, *J. Appl. Crystallogr.*, 2015, **48**, 3–10; (*c*) G. M. Sheldrick, *Acta Crystallogr.*, 2015, **A71**, 3–8; (*d*) G. M. Sheldrick, *Acta Crystallogr.*, 2015, **C71**, 3–8; (*e*) C. B. Hübschle, G. M. Sheldrick and B. Dittrich, *J. Appl. Crystallogr.*, 2011, **44**, 1281–1284, CCDC no. 2376682 (**1**) and 2376683 (**2**)†.
17 (*a*) E. R. Davidson, *J. Chem. Phys.*, 1967, **46**, 3320–3324; (*b*) K. R. Roby, *Mol. Phys.*, 1974, **27**, 789–807; (*c*) R. Heinzmann and R. Ahlrichs, *Theoret. Chim. Acta*, 1976, **42**, 33–45; (*d*) C. Erhardt and R. Ahlrichs, *Theoret. Chim. Acta*, 1985, **68**, 231–245.
18 J. P. Foster and F. Weinhold, *J. Am. Chem. Soc.*, 1980, **102**, 7211–7218.
19 (*a*) T. Lu and F. Chen, *J. Comput. Chem.*, 2012, **33**, 580–592; (*b*) H. L. Schmider and A. D. Becke, *J. Mol. Struc-THEOCHEM*, 2000, **527**, 51–61.
20 (*a*) K. B. Wiberg, *Tetrahedron*, 1968, **24**, 1083–1096; (*b*) L. K. Harper, A. L. Shoaf and C. A. Bayse, *ChemPhysChem*, 2015, **16**, 3886–3892; (*c*) I. Mayer, *J. Comput. Chem.*, 2007, **28**, 204–221.
21 (*a*) D. Kratzert, D. Leusser, J. J. Holstein, B. Dittrich, K. Abersfelder, D. Scheschkewitz and D. Stalke, *Angew. Chem., Int. Ed.*, 2013, **52**, 4478–4482; (*b*) B. Niepötter and D. Stalke, in *Organosilicon Compounds*, ed. V. Y. Lee, Academic Press, 2017, pp. 3–58.

 This journal is © The Royal Society of Chemistry 2025